ACS Catalysis

Viewpoint

pubs.acs.org/acscatalysis

Accounting for Bifurcating Pathways in the Screening for CO_2 Reduction Catalysts

Federico Calle-Vallejo*[,†,‡] and Marc T. M. Koper*[,†]

[†]Leiden Institute of Chemistry, Leiden University, P.O. Box 9502, 2300 RA Leiden, The Netherlands

[‡]Departament de Ciència de Materials i Química Fisica & Institut de Química Teòrica i Computacional (IQTCUB), Universitat de Barcelona, Martí i Franqués 1, 08028 Barcelona, Spain

Supporting Information

INTRODUCTION

In view of the innumerable interrelated variables at the nano, micro, and macro scales, existing models in catalysis do not yet fully account for the extraordinary complexity of real catalytic reactions.[1,2] For instance, consider the case of the computational screening for catalytic materials, which aims to develop rational principles for the fast and robust design of catalysts. Note that screening routines are clearly different from mechanistic studies in catalysis: for the latter, the level of detail is high while the number of analyzed materials and facets is small. Screening, on the other hand, uses a variety of assumptions to enable the simultaneous study of numerous materials.[3−7] Two of such assumptions are (1) the idea that for a given catalytic reaction a single mechanism is valid on all materials, and (2) that such materials can be represented by only one kind of sites.[3] Profuse examples attest to a great deal of development in a relatively short time in computational catalysis because of these simplifications. For instance, new catalytic materials have been designed in silico and implemented experimentally for hydrogen evolution,[8] oxygen reduction,[9−11] and water splitting,[12,13] among many others.[14] Moreover, a more fundamental outcome of these computations has been the realization that the adsorption energies of catalytic intermediates in a mechanism are governed by so-called scaling relations,[15−19] such that the qualitative features of an entire mechanism are typically described by the energy of a single intermediate, i.e. a single descriptor.

In spite of these tremendous practical and fundamental advances, materials screening for catalysis is not yet in a position to provide rapid and reliable solutions to industrial applications and it is yet to provide long-term solutions in the area of catalysis for sustainability.[20,21] Currently, a pertinent issue to tackle are the aforementioned single-mechanism and single-site assumptions, as in many real mechanisms, multiple (parallel) pathways exist that can lead to different final products. In the following, we will show a simple way of incorporating pathway bifurcation analyses in state-of-the-art materials screening routines illustrated on a particular case of current interest in catalysis, namely, the (electro)chemical reduction of CO and CO_2 to C_1 species such as methane or methanol. The withstanding debate about the reaction mechanism of this reaction[22−26] and the current difficulties in finding alloy catalysts with high activities that outperform pure metals,[27] make it a salient example to verify the applicability and impact of the single-site, single-mechanism approximations on catalytic materials design via screening.

To the best of our knowledge, studies on pathway bifurcations during CO_2/CO reduction for various metals are rare, although some examples exist.[28] Besides, there are computational studies on the structure sensitivity of specific materials: for instance, various Cu facets have been studied for the production of CH_4,[29,30] C_2H_4,[31] and CH_3CH_2OH.[32]

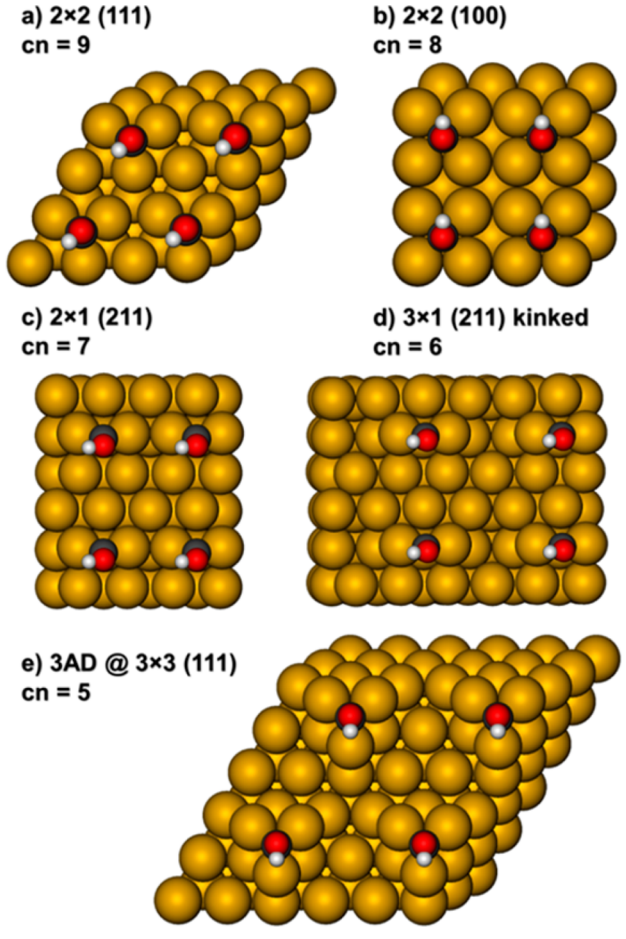

Figure 1. Active sites on nine metals (Co, Ni, Cu, Rh, Pd, Ag, Ir, Pt, Au) for three adsorbates (*CO, *COH shown in the figure, *CHO).

Received: August 28, 2017
Published: September 18, 2017

DOI: 10.1021/acscatal.7b02917
ACS Catal. 2017, 7, 7346−7351

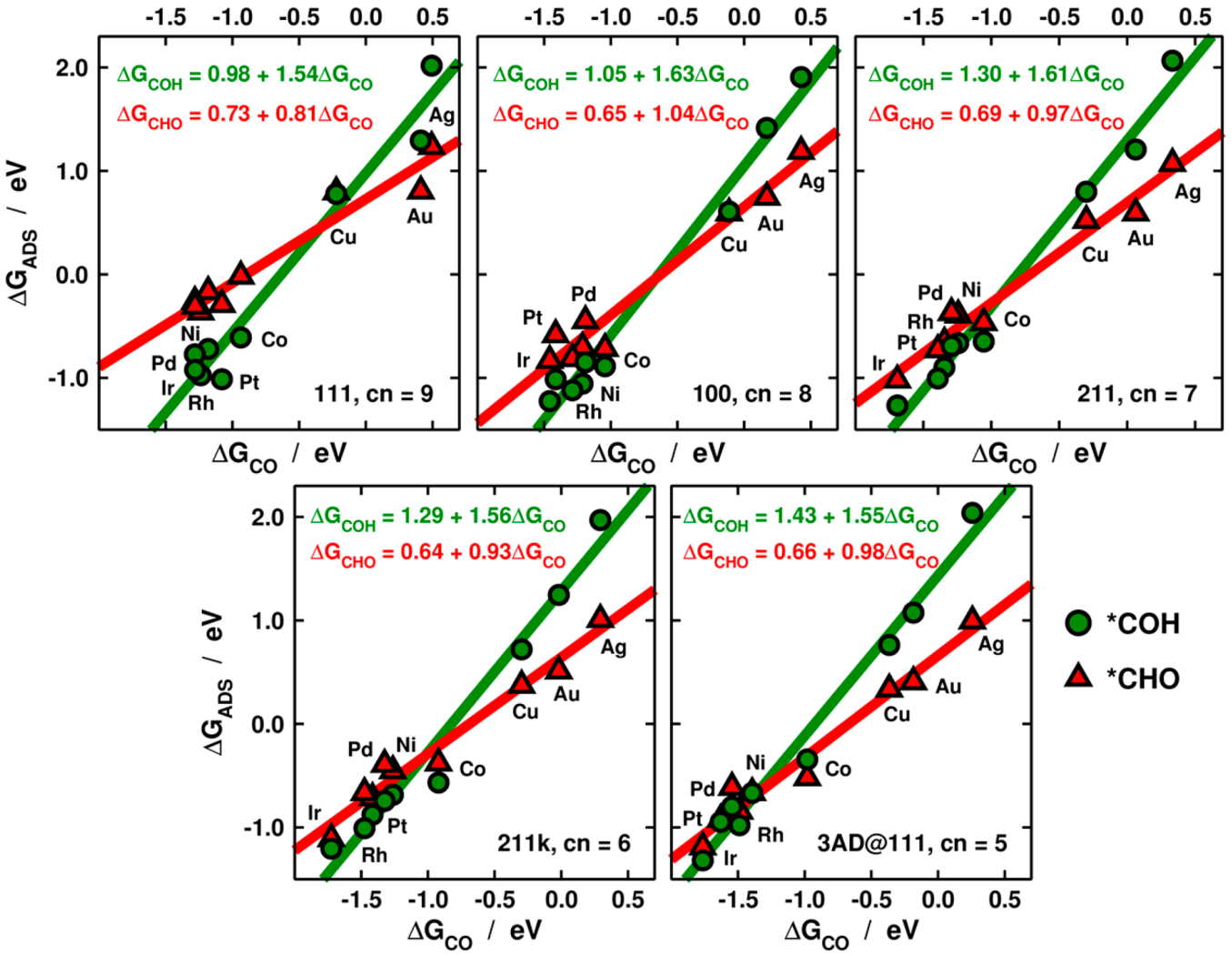

Figure 2. Universal adsorption-energy scaling relations between ΔG_{CO}, ΔG_{COH}, and ΔG_{CHO}. Every panel contains the most stable adsorption energies of the species on a given facet (see Figure 1) of nine metals, and the equations of the linear fits are provided in each case.

Various Ag[33] and Au[34] facets have also been studied for CO_2 reduction to CO. On the other hand, there exist numerous screening studies based on scaling relations for CO_2 reduction on several metals[35] and alloys[27,36] assuming a single reaction pathway. However, a simultaneous analysis of multiple materials able to systematically predict pathway bifurcations based on structural sensitivity is currently unavailable.

To illustrate this point, we will consider a canonical example of a bifurcation in pathways, often responsible for the changes in reaction selectivity, namely, the hydrogenation of *CO, considered one of the potential-limiting steps of CO and CO_2 reduction. This reaction also pertains to other important catalytic reactions such as Fischer−Tropsch synthesis and methanol synthesis.[37,38] Our computations of *CO, *CHO, and *COH on a variety of metals and structures show that universal adsorption-energy scaling relations[19] are able to predict, in simple and quantitative terms, the preferred reaction intermediates of *CO hydrogenation with chemical and structural sensitivity. This result implies that beyond the traditional use of scaling relations for the design of materials, they can also be used to systematically predict the conditions under which competing adsorbed intermediates form on any surface site of specific metals. In practical terms, our analysis shows that deviations from the single-site and single-mechanism approximations can still be rationalized by a single-descriptor approach and give hope for the development of rapid yet more accurate materials screening routines than those available today.

1. Universal Scaling Relations for *CO, *CHO, and *COH. We consider in this study the five different kinds of sites depicted in Figure 1. These sites include various terraces ((111) and (100)), edges ((211)), kinks ((211) with a missing atom at the edge, denoted (211k)) and metal adatoms (three adatoms at a (111) terrace, denoted 3AD@111), which span coordination numbers between 5 and 9 sufficient to typify the heterogeneity of a real catalyst. On each of the facets shown in Figure 1 and over the nine different transition metals studied (Co, Ni, Cu, Rh, Pd, Ag, Ir, Pt, Au), we allowed *CO, *COH and *CHO to fully relax on several adsorption sites (top, bridge, hollow) and binding modes (monodentate, bidentate). Hence, the following analysis is based on the most stable adsorption configurations, and in no case did we force the adsorbates to bind in a particular way. Furthermore, the calculations shown in Figures 2−5 for Co and Ni take into account the ferromagnetism of these two elements (see sections S1 and S2 in the Supporting Information, hereon denoted SI).

DOI: 10.1021/acscatal.7b02917
ACS Catal. 2017, 7, 7346−7351

We took the most stable adsorption energies of each adsorbate on each metal and facet to build Figure 2. The result is a plot in which it is shown that the scaling relations between the adsorption energies of *CO and *CHO (red triangles), and *CO and *COH (green circles) are universal. This means that regardless of the facet, linear correlations exist between the three sets of adsorption energies. Now, it is possible to predict and understand the values of both the slope and the offset in such scaling relations as depicted in Figure 3. The figure

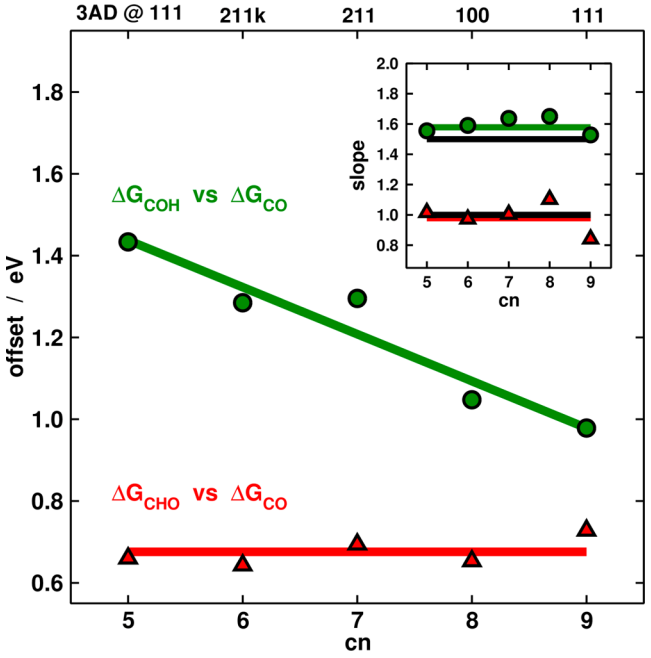

Figure 3. Structural sensitivity of the parameters of the scaling relations between ΔG_{CO}, ΔG_{COH}, ΔG_{CHO}. The values of the offset of the scaling relations in Figure 2 are shown as a function of the coordination number of the adsorption sites. For ΔG_{COH} vs ΔG_{CO} (green circles) the relationship is linear, while it is constant for ΔG_{CHO} vs ΔG_{CO} (red triangles). Inset: the slopes are independent of the coordination number of the adsorption sites. The black line marks the theoretical predictions.

collects the slopes and offsets of the linear fits in Figure 2 to understand their structural dependence. We find that a good descriptor is the coordination number of the active sites.

First of all, the inset in Figure 3 shows that the slope has a fixed value that depends on the adsorbates but not on the coordination of the active sites.[15,18,19] For *COH vs *CO, it is ~3/2, which is the ratio of the missing bonds of the carbon atoms to reach the octet (3 for *COH and 2 in the case of *CO). For *CHO vs *CO the slope is close to 1,[35] which is a reflection of two important features of *CHO: first, it is a bidentate adsorbate that typically binds to the surface via C and O. Second, the C−O double bond in unbound CHO is partially retained when adsorbed, so that the actual valence of *CHO is 2 (see further details in section S3 in the SI). The small differences between the black and red lines, and between the black and green lines in the inset of Figure 3, confirm that such bond-counting approximations to assess the slope are accurate for all facets.

Even more interesting are the trends shown in the main panel of Figure 3, which correspond to the structural dependence of the offset of the scaling relations. It is worth noting here that, as shown before for oxygenate adsorbates,[19] the offsets of scaling relations with slopes unity and nonunity behave differently. This is a consequence of the definition of the adsorption-energy scaling relation between species 1 and 2 on facet i:

$$\Delta G_{2,i} = m_{1,2}\Delta G_{1,i} + b_i \quad (1)$$

where $m_{1,2}$ and b_i are constant on facet i. If one subtracts $\Delta G_{1,i}$ on both sides of eq 1 and reorganizes, the result is

$$\Delta G_{2,i} - \Delta G_{1,i} = (m_{1,2} - 1)\Delta G_{1,i} + b_i \quad (2)$$

According to eq 2, if $m_{1,2} = 1$ the term $\Delta G_{2,i} - \Delta G_{1,i}$ is constant and equal to the offset, whereas if $m_{1,2} \neq 1$ then $\Delta G_{2,i} - \Delta G_{1,i}$ is not constant and depends on $\Delta G_{1,i}$ (which typically become more negative as the surface coordination is lowered[11,19]) and $m_{1,2}$. Therefore, for *COH vs *CO (slope ~1.5), the offsets vary linearly with coordination number, whereas they are constant for *CHO vs *CO (slope ~1).

2. Including Pathway Bifurcation in Scaling-Relations-Based Screening Routines. From a computational chemistry standpoint, Figure 3 is a new and useful extension to carbon-bound adsorbates of previous findings pertaining to oxygenate species.[19] Furthermore, we have intentionally provided in Figures 1−3 approximate free energies (section S1 in the SI) instead of mere DFT energies to be able to inspect the implications of such universal scaling relations in catalysis.

Note that the most widespread reaction pathway for the electrocatalytic reduction of CO/CO_2 considers that Cu and many other transition metals form the intermediate *CHO upon *CO hydrogenation.[22,29,35] Since the offset is constant

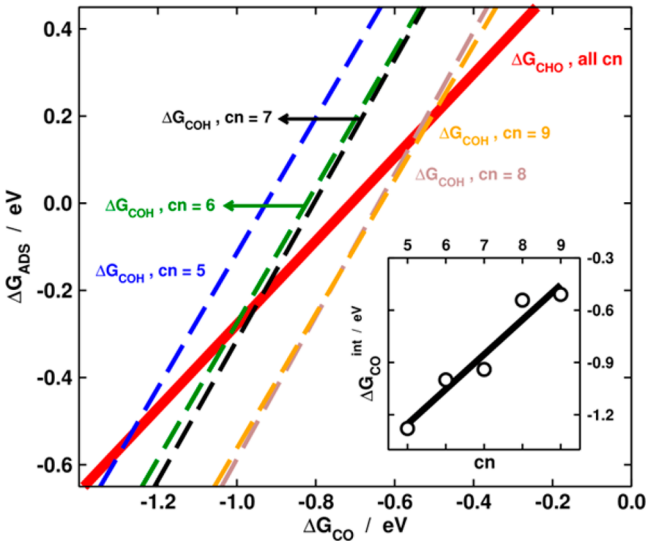

Figure 4. Structure-sensitive determination of pathway bifurcation using the data in Figure 2: a single line represents ΔG_{CHO} vs ΔG_{CO} and several lines represent ΔG_{COH} vs ΔG_{CO}. Inset: *CO adsorption energies at the intersection points (ΔG_{CO}^{int}) depend linearly on the site's coordination. For a given facet, metals with $\Delta G_{CO} > \Delta G_{CO}^{int}$ form *CHO, those with $\Delta G_{CO} < \Delta G_{CO}^{int}$ form *COH.

across materials and facets, as shown in Figure 3, it is currently believed that such a constant separation is one of the main reasons for the high overpotential for the reduction of CO/CO_2 to more reduced products such as methane or methanol. Therefore, it is widely accepted that breaking the scaling relation between *CO and *CHO may help decrease the overpotential.[39,40] However, before trying to break a scaling

DOI: 10.1021/acscatal.7b02917
ACS Catal. 2017, 7, 7346−7351

relation, which is an experimental and computational tour de force, it is pertinent to ask whether the involved adsorbates are indeed the true reaction intermediates on every metal and facet. We solve here this paramount question with the help of universal scaling relations.

We have condensed in Figure 4 the linear fits of the trends in Figure 2. The figure shows that a single line describing the trends in adsorption energies of *CHO vs *CO is intersected at various adsorption energies by the lines that represent the trends for *COH vs *CO. From a mechanistic perspective, Figure 4 shows that it is possible to predict on a per-metal and per-facet basis whether a given reaction intermediate is likely to form or not. In other words, this simple plot and its inset enable the structure- and chemically sensitive prediction of reaction pathways. This is a new application of scaling relations, which are typically used in materials screening to build routines in which the reaction of interest proceeds identically on all materials.[7,9,11,13,16,25,29,35,39,40]

The inset of Figure 4 shows the *CO adsorption energies per facet that determine the relative favorability of a given intermediate (denoted ΔG^{int}_{CO}). These values are the *CO adsorption energies at which the lines intersect, and as such they also depend linearly on the coordination number of the active sites.

3. Implications for CO_2 Reduction Design Principles of Incorporating Pathway Bifurcation into Screening Routines. Using Figure 4, one can build structure- and chemically sensitive maps of reaction intermediates indicating the thermodynamically most stable adsorbed intermediates and products of a given reaction, as illustrated in Table 1. From this table, we conclude that generally the most abundant reaction intermediate of *CO hydrogenation is *COH. Only Cu, Ag, and Au tend to form *CHO. Besides, for several metals such as Cu, Ag, and Co, *COH and *CHO coexist depending on the coordination number of the active sites. Therefore, while indeed a constant energetic separation exists between *CO and *CHO (see Figures 2−4), its supposed pervasive and harmful effect on the overpotential needs to be rethought: for Cu, Ag, and Au, it is fine to assume that CO reduction proceeds via *CHO, but on Co, Rh, Ir, Ni, Pd, and Pt, it proceeds via *COH, in line with Janik and co-workers' observations.[28] More importantly, since *CHO and *COH bind differently to the substrates, design strategies aimed at enhancing catalytic activities by modifying *CHO binding can alter *COH binding only fortuitously.

Table 1. Most Stable Adsorbates Formed upon the First Hydrogenation of CO[a]

metal	111 cn =9	100 cn = 8	211 cn = 7	211k cn = 6	3AD@111 cn = 5
Co	*COH	*COH	*COH	*COH	*CHO
Rh	*COH	*COH	*COH	*COH	*COH
Ir	*COH	*COH	*COH	both	*COH
Ni	*COH	*COH	*COH	*COH	both
Pd	*COH	*COH	*COH	*COH	*COH
Pt	*COH	*COH	*COH	*COH	both
Cu	both	both	*CHO	*CHO	*CHO
Ag	*CHO	*CHO	*CHO	*CHO	*CHO
Au	*CHO	*CHO	*CHO	*CHO	*CHO

[a]In case the difference between the adsorption energies of *COH and *CHO differ by less than 0.1 eV, both intermediates are reported.

Another important aspect of *CO hydrogenation is that it is believed to be the potential-limiting step of CO/CO_2 reduction to methane.[22,29,35] The onset potentials (denoted U_L) are calculated as the reaction energy or potential of the potential-limiting step,[22,41] in this case either $*CO + H^+ + e^- \rightarrow *CHO$ or $*CO + H^+ + e^- \rightarrow *COH$.

Figure 5 shows the potentials of CO hydrogenation for the nine metals under study, several of which are between 0 and −0.5 V_{RHE}. Given the large overpotentials observed experimentally for CO/CO_2 reduction on transition metals,[25,26] we conclude that *CO hydrogenation is likely not the potential-limiting step of this reaction on the majority of these multifaceted metals, except perhaps for those with 11 valence electrons (especially Cu and Ag). This suggests that breaking the scaling relationship between the adsorption energies of *CHO vs *CO is probably not the key to design enhanced CO/CO_2 reduction metal catalysts.

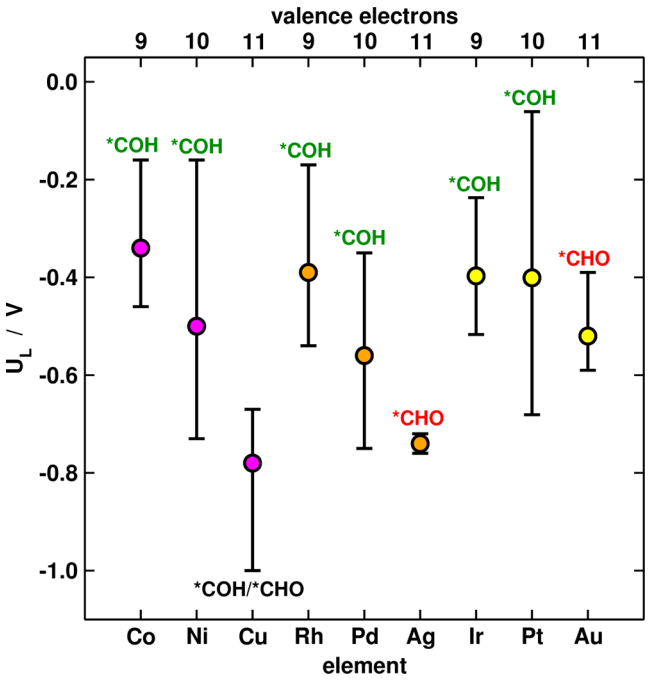

Figure 5. Electrochemical potentials required for *CO hydrogenation. The values reported are either for *COH or *CHO formation, according to Table 1. We also indicate for each metal the most likely adsorbate, based on Table 1. The circles correspond to the per-metal average of the five potentials obtained for the sites in Figure 1. The error bars correspond to the ranges spanned by such potentials.

Although we have used here well-known solvation corrections for *CO, *CHO, and *COH,[22,42] Janik and co-workers[28] recently pointed out that adsorbate solvation can substantially influence pathway bifurcation. Therefore, in the SI, section S4, we complement Table 1 and Figure 5 with the analysis of two additional cases: one in which the three adsorbates are identically solvated (i.e., either *COH is less solvated than expected or *CO and *CHO are more solvated) and another in which *COH is more solvated than expected.

DOI: 10.1021/acscatal.7b02917
ACS Catal. 2017, 7, 7346−7351

The first scenario largely favors *CHO formation and makes U_L more negative with respect to the values in Figure 5. The latter scenario favors *COH formation and makes U_L less negative compared to the values in Figure 5.

CONCLUDING REMARKS

Current computational screening techniques based on scaling relations in heterogeneous catalysis work on the basis of two main simplifications: all catalysts follow a single mechanism involving the same intermediates and products, and such catalysts are represented by only one of their active sites. However, real catalytic mechanisms regularly involve bifurcations between pathways. Using the hydrogenation of *CO to *CHO and *COH as a case study, we have shown here that materials design routines incorporating universal scaling relations are able to account for the intuitive yet missing ingredient in materials screening that catalytic reactions frequently proceed via different adsorbed intermediates depending on the chemical and structural nature of the active sites. The essence of the predictability of the bifurcation in reaction pathways lies in the different slopes and offsets of the *COH vs *CO and the *CHO vs *CO scaling relations, and these parameters can be understood on the basis of simple concepts of chemical bonding. A complete screening routine considering metal- and facet-dependent pathways is at hand following the approach given here.

We emphasize that catalytic models of a reaction on a single material are generally much more detailed than screening studies. For the latter, a compromise needs to be made with regards to rigorousness so as to enable the study of a large number of materials. Among others, further developments in materials screening should include the joint analysis on the adsorption energies of coverage effects,[43−45] solvation effects,[28,46−49] and exchange-correlation-associated errors on gas-phase and adsorbed intermediates,[28,50,51] together with transition-state considerations.[23,52,53] To date, no screening routine based on scaling relations incorporates all those effects.

The particular implication of our analysis for the electrocatalytic reduction of CO/CO_2 is that the common assumption that *CO hydrogenation is the potential-limiting step does not apply to most metals, other than copper. As a result, the most likely intermediate on transition metals is *COH and not *CHO (see also ref 28), and the prevalence of one or other intermediate depends on the chemical nature and coordination number of the active sites in a systematic way. These insights illustrate that the power of scaling relations in catalysis extends beyond the prediction of the most active catalyst for a particular single pathway; it also enables the rationalization of bifurcating pathways, which so far have remained underexposed in catalyst design via screening.

ASSOCIATED CONTENT

Supporting Information

The Supporting Information is available free of charge on the ACS Publications website at DOI: 10.1021/acscatal.7b02917.

Computational methods, spin polarization effects on adsorption-energy scaling relations, origin of the unity slope for the scaling relationship of *CO vs *CHO, solvation effects on pathway bifurcation (PDF)

AUTHOR INFORMATION

Corresponding Authors

*F.C.-V.: f.calle.vallejo@chem.leidenuniv.nl.

*M.T.M.K.: m.koper@chem.leidenuniv.nl.

ORCID

Federico Calle-Vallejo: 0000-0001-5147-8635

Marc T. M. Koper: 0000-0001-6777-4594

Notes

The authors declare no competing financial interest.

ACKNOWLEDGMENTS

F.C.V. acknowledges funding from The Netherlands Organization for Scientific Research (NWO), Veni project number 722.014.009. The use of supercomputing facilities at SURFsara was sponsored by NWO Physical Sciences, with financial support by NWO. F.C.V. also thanks Spanish MEC for a Ramón y Cajal research contract (RYC-2015-18996).

REFERENCES

(1) Vlachos, D. G. In *Advances in Chemical Engineering*, Guy, B. M., Ed.; Academic Press: San Diego, 2005; Vol. *30*, pp 1−61.

(2) Jahnke, T.; Futter, G.; Latz, A.; Malkow, T.; Papakonstantinou, G.; Tsotridis, G.; Schott, P.; Gérard, M.; Quinaud, M.; Quiroga, M.; Franco, A. A.; Malek, K.; Calle-Vallejo, F.; Ferreira de Morais, R.; Kerber, T.; Sautet, P.; Loffreda, D.; Strahl, S.; Serra, M.; Polverino, P.; Pianese, C.; Mayur, M.; Bessler, W. G.; Kompis, C. *J. Power Sources* **2016**, *304*, 207−233.

(3) Norskov, J. K.; Bligaard, T.; Rossmeisl, J.; Christensen, C. H. *Nat. Chem.* **2009**, *1*, 37−46.

(4) Van Santen, R. A. *Acc. Chem. Res.* **2009**, *42*, 57−66.

(5) Wang, Z.; Hu, P. *Philos. Trans. R. Soc., A* **2016**, *374*, 20150085.

(6) Reuter, K.; Plaisance, C. P.; Oberhofer, H.; Andersen, M. *J. Chem. Phys.* **2017**, *146*, 040901.

(7) Calle-Vallejo, F.; Koper, M. T. M. *Electrochim. Acta* **2012**, *84*, 3−11.

(8) Greeley, J.; Jaramillo, T. F.; Bonde, J.; Chorkendorff, I.; Norskov, J. K. *Nat. Mater.* **2006**, *5*, 909−913.

(9) Greeley, J.; Stephens, I. E. L.; Bondarenko, A. S.; Johansson, T. P.; Hansen, H. A.; Jaramillo, T. F.; Rossmeisl, J.; Chorkendorff, I.; Nørskov, J. K. *Nat. Chem.* **2009**, *1*, 552−556.

(10) Siahrostami, S.; Verdaguer-Casadevall, A.; Karamad, M.; Deiana, D.; Malacrida, P.; Wickman, B.; Escudero-Escribano, M.; Paoli, E. A.; Frydendal, R.; Hansen, T. W.; Chorkendorff, I.; Stephens, I. E. L.; Rossmeisl, J. *Nat. Mater.* **2013**, *12*, 1137−1143.

(11) Calle-Vallejo, F.; Tymoczko, J.; Colic, V.; Vu, Q. H.; Pohl, M. D.; Morgenstern, K.; Loffreda, D.; Sautet, P.; Schuhmann, W.; Bandarenka, A. S. *Science* **2015**, *350*, 185.

(12) Halck, N. B.; Petrykin, V.; Krtil, P.; Rossmeisl, J. *Phys. Chem. Chem. Phys.* **2014**, *16*, 13682−13688.

(13) Diaz-Morales, O.; Ledezma-Yanez, I.; Koper, M. T. M.; Calle-Vallejo, F. *ACS Catal.* **2015**, *5*, 5380−5387.

(14) Seh, Z. W.; Kibsgaard, J.; Dickens, C. F.; Chorkendorff, I.; Nørskov, J. K.; Jaramillo, T. F. *Science* **2017**, *355*, eaad4998.

(15) Abild-Pedersen, F.; Greeley, J.; Studt, F.; Rossmeisl, J.; Munter, T. R.; Moses, P. G.; Skúlason, E.; Bligaard, T.; Nørskov, J. K. *Phys. Rev. Lett.* **2007**, *99*, 016105.

(16) Montemore, M. M.; Medlin, J. W. *Catal. Sci. Technol.* **2014**, *4*, 3748−3761.

(17) Su, H.-Y.; Sun, K.; Wang, W.-Q.; Zeng, Z.; Calle-Vallejo, F.; Li, W.-X. *J. Phys. Chem. Lett.* **2016**, *7*, 5302−5306.

(18) Calle-Vallejo, F.; Martinez, J. I.; Garcia-Lastra, J. M.; Rossmeisl, J.; Koper, M. T. M. *Phys. Rev. Lett.* **2012**, *108*, 116103.

(19) Calle-Vallejo, F.; Loffreda, D.; Koper, M. T. M.; Sautet, P. *Nat. Chem.* **2015**, *7*, 403−410.

(20) Lewis, N. S.; Nocera, D. G. *Proc. Natl. Acad. Sci. U. S. A.* **2006**, *103*, 15729−15735.

DOI: 10.1021/acscatal.7b02917
ACS Catal. 2017, 7, 7346−7351

(21) Vesborg, P. C. K.; Jaramillo, T. F. *RSC Adv.* **2012**, *2*, 7933−7947.
(22) Peterson, A. A.; Abild-Pedersen, F.; Studt, F.; Rossmeisl, J.; Norskov, J. K. *Energy Environ. Sci.* **2010**, *3*, 1311−1315.
(23) Nie, X.; Esopi, M. R.; Janik, M. J.; Asthagiri, A. *Angew. Chem., Int. Ed.* **2013**, *52*, 2459−2462.
(24) Xiao, H.; Cheng, T.; Goddard, W. A. *J. Am. Chem. Soc.* **2017**, *139*, 130−136.
(25) Kortlever, R.; Shen, J.; Schouten, K. J. P.; Calle-Vallejo, F.; Koper, M. T. M. *J. Phys. Chem. Lett.* **2015**, *6*, 4073−4082.
(26) Gattrell, M.; Gupta, N.; Co, A. *J. Electroanal. Chem.* **2006**, *594*, 1−19.
(27) Jovanov, Z. P.; Hansen, H. A.; Varela, A. S.; Malacrida, P.; Peterson, A. A.; Nørskov, J. K.; Stephens, I. E. L.; Chorkendorff, I. *J. Catal.* **2016**, *343*, 215−231.
(28) Akhade, S. A.; Luo, W.; Nie, X.; Asthagiri, A.; Janik, M. J. *Catal. Sci. Technol.* **2016**, *6*, 1042−1053.
(29) Durand, W. J.; Peterson, A. A.; Studt, F.; Abild-Pedersen, F.; Nørskov, J. K. *Surf. Sci.* **2011**, *605*, 1354−1359.
(30) Luo, W.; Nie, X.; Janik, M. J.; Asthagiri, A. *ACS Catal.* **2016**, *6*, 219−229.
(31) Li, H.; Li, Y.; Koper, M. T. M.; Calle-Vallejo, F. *J. Am. Chem. Soc.* **2014**, *136*, 15694−15701.
(32) Ledezma-Yanez, I.; Gallent, E. P.; Koper, M. T. M.; Calle-Vallejo, F. *Catal. Today* **2016**, *262*, 90−94.
(33) Rosen, J.; Hutchings, G. S.; Lu, Q.; Rivera, S.; Zhou, Y.; Vlachos, D. G.; Jiao, F. *ACS Catal.* **2015**, *5*, 4293−4299.
(34) Zhu, W.; Zhang, Y.-J.; Zhang, H.; Lv, H.; Li, Q.; Michalsky, R.; Peterson, A. A.; Sun, S. *J. Am. Chem. Soc.* **2014**, *136*, 16132−16135.
(35) Peterson, A. A.; Nørskov, J. K. *J. Phys. Chem. Lett.* **2012**, *3*, 251−258.
(36) Hansen, H. A.; Shi, C.; Lausche, A. C.; Peterson, A. A.; Norskov, J. K. *Phys. Chem. Chem. Phys.* **2016**, *18*, 9194−9201.
(37) Huber, G. W.; Iborra, S.; Corma, A. *Chem. Rev.* **2006**, *106*, 4044−4098.
(38) Van Der Laan, G. P.; Beenackers, A. A. C. M. *Catal. Rev.: Sci. Eng.* **1999**, *41*, 255−318.
(39) Li, Y.; Sun, Q. *Adv. Energy Mater.* **2016**, *6*, 1600463.
(40) Hong, X.; Chan, K.; Tsai, C.; Nørskov, J. K. *ACS Catal.* **2016**, *6*, 4428−4437.
(41) Nørskov, J. K.; Rossmeisl, J.; Logadottir, A.; Lindqvist, L.; Kitchin, J. R.; Bligaard, T.; Jónsson, H. *J. Phys. Chem. B* **2004**, *108*, 17886−17892.
(42) Calle-Vallejo, F.; Koper, M. T. M. *Angew. Chem., Int. Ed.* **2013**, *52*, 7282−7285.
(43) Akhade, S. A.; Luo, W.; Nie, X.; Bernstein, N. J.; Asthagiri, A.; Janik, M. J. *Phys. Chem. Chem. Phys.* **2014**, *16*, 20429−20435.
(44) Grabow, L. C.; Hvolbæk, B.; Nørskov, J. K. *Top. Catal.* **2010**, *53*, 298−310.
(45) Katsounaros, I.; Figueiredo, M. C.; Chen, X.; Calle-Vallejo, F.; Koper, M. T. M. *ACS Catal.* **2017**, *7*, 4660−4667.
(46) Calle-Vallejo, F.; Krabbe, A.; Garcia-Lastra, J. M. *Chem. Sci.* **2017**, *8*, 124−130.
(47) He, Z.-D.; Hanselman, S.; Chen, Y.-X.; Koper, M. T. M.; Calle-Vallejo, F. *J. Phys. Chem. Lett.* **2017**, *8*, 2243−2246.
(48) Kolb, M. J.; Farber, R. G.; Derouin, J.; Badan, C.; Calle-Vallejo, F.; Juurlink, L. B. F.; Killelea, D. R.; Koper, M. T. M. *Phys. Rev. Lett.* **2016**, *116*, 136101.
(49) Kolb, M. J.; Wermink, J.; Calle-Vallejo, F.; Juurlink, L. B. F.; Koper, M. T. M. *Phys. Chem. Chem. Phys.* **2016**, *18*, 3416−3422.
(50) Christensen, R.; Hansen, H. A.; Vegge, T. *Catal. Sci. Technol.* **2015**, *5*, 4946−4949.
(51) Briquet, L. G. V.; Sarwar, M.; Mugo, J.; Jones, G.; Calle-Vallejo, F. *ChemCatChem* **2017**, *9*, 1261−1268.
(52) Bligaard, T.; Nørskov, J. K.; Dahl, S.; Matthiesen, J.; Christensen, C. H.; Sehested, J. *J. Catal.* **2004**, *224*, 206−217.
(53) Sutton, J. E.; Vlachos, D. G. *J. Catal.* **2016**, *338*, 273−283.

DOI: 10.1021/acscatal.7b02917
ACS Catal. 2017, 7, 7346−7351